



## Digital Receipt

This receipt acknowledges that Turnitin received your paper. Below you will find the receipt information regarding your submission.

The first page of your submissions is displayed below.

Submission author: Bernadeta Wuri Harini  
Assignment title: Periksa similarity  
Submission title: The Effect of Motor Parameters on the Induction Motor Spee...  
File name: or\_Speed\_Sensorless\_Control\_System\_using\_Luenberger\_Ob...  
File size: 757.73K  
Page count: 16  
Word count: 3,093  
Character count: 15,702  
Submission date: 19-Aug-2022 09:31AM (UTC+0700)  
Submission ID: 1884178139

International Journal of Applied Sciences and Smart Technologies  
Volume 4, Issue 1, pages 59-74  
p-ISSN 2655-8564, e-ISSN 2685-9432

### The Effect of Motor Parameters on the Induction Motor Speed Sensorless Control System using Luenberger Observer

Bernadeta Wuri Harini<sup>1,\*</sup>

<sup>1</sup> Department of Electrical Engineering, Sanata Dharma University,  
Yogyakarta, Indonesia  
\*Corresponding Author: wuribernard@usd.ac.id

(Received 08-04-2022; Revised 27-05-2022; Accepted 29-05-2022)

#### Abstract

The sensorless control system is a control system without a controlled variable sensor. The controlled variable is estimated using an observer. In this investigation, the sensorless control system is used to control induction motor speed. The observer that is used is the Luenberger observer. One of the drawbacks of the sensorless control system is precision motor parameter values. In this research, the effect of induction motor parameters in a speed sensorless control system, i.e. resistance and inductance motor, will be investigated. The differences in induction motor parameters between the controller and the actual value affect the system response. The value differences of  $R_r$  and  $R_s$  that can be applied are a maximum of 50%. However, the small differences in the inductance value greatly affect the system response. To get a good response, the value differences of  $L_s$  and  $L_r$  are between -5% to +5%, while the difference in the value of  $L_m$  is between -3% to +3%.



59

This work is licensed under a [Creative Commons Attribution 4.0 International License](https://creativecommons.org/licenses/by/4.0/).

# The Effect of Motor Parameters on the Induction Motor Speed Sensorless Control System using Luenberger Observer

*by Harini Bernadeta Wuri*

---

**Submission date:** 19-Aug-2022 09:31AM (UTC+0700)

**Submission ID:** 1884178139

**File name:** or\_Speed\_Sensorless\_Control\_System\_using\_Luenberger\_Observer.pdf (757.73K)

**Word count:** 3093

**Character count:** 15702

## **The Effect of Motor Parameters on the Induction Motor Speed Sensorless Control System using Luenberger Observer**

Bernadeta Wuri Harini<sup>1,\*</sup>

<sup>1</sup> *Department of Electrical Engineering, Sanata Dharma University,  
Yogyakarta, Indonesia*

*\*Corresponding Author: [wuribernard@usd.ac.id](mailto:wuribernard@usd.ac.id)*

(Received 08-04-2022; Revised 27-05-2022; Accepted 29-05-2022)

### **Abstract**

The sensorless control system is a control system without a controlled variable sensor. The controlled variable is estimated using an observer. In this investigation, the sensorless control system is used to control induction motor speed. The observer that is used is the Luenberger observer. One of the drawbacks of the sensorless control system is precision motor parameter values. In this research, the effect of induction motor parameters in a speed sensorless control system, i.e. resistance and inductance motor, will be investigated. The differences in induction motor parameters between the controller and the actual value affect the system response. The value differences of  $R_r$  and  $R_s$  that can be applied are a maximum of 50%. However, the small differences in the inductance value greatly affect the system response. To get a good response, the value differences of  $L_s$  and  $L_r$  are between -5% to +5%, while the difference in the value of  $L_m$  is between -3% to +3%.



**Keywords:** inductance, induction motor, Luenberger observer, resistance, sensorless

## 1 Introduction

A control system without a controlled variable sensor, often known as "sensorless control," is one controller that is still being researched. Sensorless control systems evolved to overcome the challenges of sensor installation that sensor-based control systems faced. Sensor-based control systems are widely used by researchers, such as those of Z. Alpholichy X., et al [1] and Y. E. Loho, et al [2]. Sensors will drive up prices and complicate installation [3]. The controlled variable in this system is approximated from the plant's current input using an observer rather than being measured directly by a sensor [4]. The stator current is used to estimate the motor speed using an observer. Sensorless control will be used to control the speed of the Induction Motor in this investigation.

The induction motor is one of the Alternating Current (AC) motors. The phase angle, as well as the modulo current (current vector), must be controlled while driving an AC motor [4]. It is not the same as a DC motor. The torque and flux that produce the AC motor current are decoupled in vector control so that they can be controlled independently.

Precision motor parameter values are one of the drawbacks of the sensorless control approach for controlling motor speed. For this sensorless speed control to work properly, parameter values must be clearly understood. As a result, a variety of approaches for determining induction motor parameter values have been offered by different researchers [5][6]. The importance of induction motor parameters is also underlined in the paper[7]. The disparity in parameter values causes inaccuracies in motor speed, according to this article. However, it is not indicated in these trials how much variances in motor parameter values will affect the speed controller. A motor speed error will occur if the motor parameters deviate from the real parameter [8]. In that research, it is used MRAS observer to estimate the Permanent Magnet Synchronous Motor (PMSM).

## 2 Research Methodology

### 2.1. Induction Motor Sensorless Control System

The diagram illustrates the control architecture for an induction motor. It starts with a reference speed  $\omega_r^*$  which is compared with the actual speed  $\hat{\omega}$  to produce a speed error. This error is processed by a 'Speed Controller IP' block to generate a reference d-axis current  $i_{sd}^*$ . This reference current is then compared with the actual d-axis current  $i_{sd}$  to produce a current error. This error is processed by a 'Current Controller' block to generate a reference q-axis current  $i_{sq}^*$ . This reference current is then compared with the actual q-axis current  $i_{sq}$  to produce another current error. This error is processed by a 'Decoupling' block to generate a reference d-axis voltage  $u_{sd}$  and a reference q-axis voltage  $u_{sq}$ . These reference voltages are then compared with the actual d-axis voltage  $v_{sd}$  and q-axis voltage  $v_{sq}$  to produce voltage errors. These voltage errors are processed by a 'dq/abc' converter block to generate reference phase voltages  $v_a$ ,  $v_b$ , and  $v_c$ . These reference voltages are then compared with the actual phase voltages  $v_a$ ,  $v_b$ , and  $v_c$  to produce voltage errors. These voltage errors are processed by a 'PWM' block to generate a PWM signal. This PWM signal is then compared with the actual PWM signal to produce a PWM error. This PWM error is processed by an 'Inverter' block to generate the final PWM signal. This final PWM signal is then compared with the actual PWM signal to produce a PWM error. This PWM error is processed by an 'Induction Motor (M)' block to generate the final output. The final output is then compared with the reference speed  $\omega_r^*$  to produce a speed error, which is fed back to the 'Speed Controller IP' block. The 'Luenberger' block is used to estimate the actual speed  $\hat{\omega}$  from the reference speed  $\omega_r^*$  and the speed error.

### 2.1.1. Induction Motor Mathematic Model

$$\begin{bmatrix} v_{sa} \\ v_{sb} \\ v_0 \end{bmatrix} = \sqrt{\frac{2}{3}} \begin{bmatrix} 1 & -\frac{1}{2} & -\frac{1}{2} \\ 0 & \frac{\sqrt{3}}{2} & -\frac{\sqrt{3}}{2} \\ \frac{1}{2} & \frac{1}{2} & \frac{1}{2} \end{bmatrix} \begin{bmatrix} v_{sa} \\ v_{sb} \\ v_{sc} \end{bmatrix} \quad (1)$$

61

The Park transformation transforms a stationary reference frame into a rotating reference ( $d, q, 0$ ) frame using the equation

$$\begin{bmatrix} v_{sd} \\ v_{sq} \end{bmatrix} = \begin{bmatrix} \cos \theta_e & \sin \theta_e \\ -\sin \theta_e & \cos \theta_e \end{bmatrix} \begin{bmatrix} v_{sa} \\ v_{s\beta} \end{bmatrix} \quad (2)$$

where  $\theta_e$  is the electric angle of the motor, while  $V_{sd}$  and  $V_{sq}$  are the stator voltage in  $d$ - $q$  reference frame.

The induction motor mathematical model in  $d$ - $q$  frame [10] is

$$\frac{d}{dt} i_{sd} = \frac{1}{\sigma L_s} V_{sd} - \left( \frac{R_s}{\sigma L_s} + \frac{(1-\sigma)}{\sigma \tau_r} \right) i_{sd} + \frac{(1-\sigma)}{\sigma \tau_r} i_{rd} + \frac{(1-\sigma) N_p \omega_r}{\sigma} i_{rq} + \omega_e i_{sq} \quad (3)$$

$$\frac{d}{dt} i_{sq} = \frac{1}{\sigma L_s} V_{sq} - \left( \frac{R_s}{\sigma L_s} + \frac{(1-\sigma)}{\sigma \tau_r} \right) i_{sq} + \frac{(1-\sigma)}{\sigma \tau_r} i_{rq} + \frac{(1-\sigma) N_p \omega_r}{\sigma} i_{rd} + \omega_e i_{sd} \quad (4)$$

$$\frac{d}{dt} i_{rd} = -\frac{R_r}{L_r} i_{rd} + \frac{R_r}{L_r} i_{sd} + (\omega_e - N_p \omega_r) i_{rq} \quad (5)$$

$$\frac{d}{dt} i_{rq} = -\frac{R_r}{L_r} i_{rq} + \frac{R_r}{L_r} i_{sq} - (\omega_e - N_p \omega_r) i_{rd} \quad (6)$$

$$\frac{d}{dt} \theta_e = N_p \omega_r + \frac{i_{sq}}{\tau_r i_{mr}} \quad (7)$$

$$\frac{d}{dt} \omega_r = \frac{1}{J} (T_e - T_L - B \cdot \omega_r) \quad (8)$$

$$\frac{d}{dt} \theta_r = \omega_r \quad (9)$$

Where  $i_{sd}$  is stator current in  $d$ -frame,  $i_{sq}$  is stator current in  $q$ -frame,  $i_{rd}$  is rotor current in  $d$ -frame,  $i_{rq}$  is rotor current in  $q$ -frame,  $\theta_e$  is voltage vector angle, and  $\omega_r$  is rotor speed.

Table 1 shows the parameter values of the induction motor that is used in this paper. The parameters are shown in Figure 2 [11].

Table 1. Parameter Values of Induction Motor

Symbol	Description	Values	Unit
$N_p$	Pole pairs	2	pairs
$R_r$	Rotor resistance	2.9	$\Omega$
$R_s$	Stator resistance	2.76	$\Omega$
$L_s$	Stator inductance	0.2349	H
$L_r$	Rotor inductance	0.2349	H
$L_m$	Mutual inductance	0.2279	H

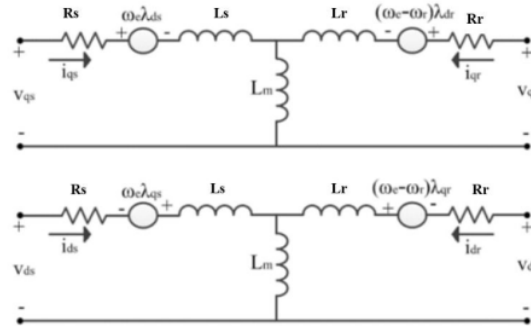


Figure 2. Equivalent Circuit in  $d$ - $q$  frame

### 2.1.2. Observer Luenberger

Luenberger observer is one of observer that uses adaptive method to estimate the controlled variable [12]. The equations of the estimation [10] are

$$\frac{d}{dt} \hat{i}_{sd} = -\left(\frac{R_s}{\sigma L_s} + \frac{(1-\sigma)}{\sigma \tau_r}\right) \hat{i}_{sd} + \omega_e \hat{i}_{sq} + \frac{L_m}{\sigma L_s L_r \tau_r} \hat{\phi}_{rd} + \frac{L_m N_p \omega_r}{\sigma L_s L_r} \hat{\phi}_{rq} + \frac{1}{\sigma L_s} v_{sd} + g_1 (i_{sd} - \hat{i}_{sd}) - g_2 (i_{sq} - \hat{i}_{sq}) \quad (10)$$

$$\frac{d}{dt} \hat{i}_{sq} = -\omega_e \hat{i}_{sd} + \frac{1}{\sigma L_s} \left(-R_s - \frac{L_m^2}{\tau_r L_r}\right) \hat{i}_{sq} - \frac{L_m N_p \omega_r}{\sigma L_s L_r} \hat{\phi}_{rd} + \frac{L_m}{\sigma L_s L_r \tau_r} \hat{\phi}_{rq} + \frac{1}{\sigma L_s} v_{sq} + g_2 (i_{sd} - \hat{i}_{sd}) + g_1 (i_{sq} - \hat{i}_{sq}) \quad (11)$$

$$\frac{d}{dt} \hat{\psi}_{rd} = \frac{R_r}{L_r} L_m \hat{i}_{sd} - \frac{1}{\tau_r} \hat{\phi}_{rd} + (\omega_e - N_p \omega_r) \hat{\phi}_{rq} + g_3 (i_{sd} - \hat{i}_{sd}) - g_4 (i_{sq} - \hat{i}_{sq}) \quad (12)$$

$$\frac{d}{dt} \hat{\psi}_{rq} = \frac{L_m}{\tau_r} \hat{i}_{sq} - (\omega_e - N_p \omega_r) \hat{\phi}_{rd} + \frac{1}{\tau_r} \hat{\phi}_{rq} + g_4 (i_{sd} - \hat{i}_{sd}) + g_3 (i_{sq} - \hat{i}_{sq}) \quad (13)$$

where

$$g_1 = \frac{(k-1)}{k} \left(-\frac{R_s}{\sigma L_s} - \frac{R_r}{\sigma L_r}\right) \quad (14)$$

$$g_2 = -\frac{(k-1)}{k} N_p \omega_r \quad (15)$$

$$g_3 = \frac{(k-1)}{k(\tau_r^2 N_p^2 \hat{\omega}_r^2 + 1)} \left(\frac{R_s R_r \tau_r + L_s R_r - \sigma \tau_r L_s L_r N_p^2 \hat{\omega}_r^2}{L_m}\right) \quad (16)$$

$$g_4 = \frac{(k-1)}{k(\tau_r^2 N_p^2 \hat{\omega}_r^2 + 1)} \left(\frac{(R_s L_r \tau_r + L_s R_r \tau_r - \sigma L_s L_r) N_p^2 \hat{\omega}_r}{L_m}\right) \quad (17)$$

The estimation speed ( $\hat{\omega}_r$ ) is then calculated using equation

$$\hat{\omega}_r = K_p(\hat{\psi}_{rq}e_{isd} - \hat{\psi}_{rd}e_{isq}) + K_i \int (\hat{\psi}_{rq}e_{isd} - \hat{\psi}_{rd}e_{isq})dt \quad (18)$$

where

$$e_{isd} = i_{sd} - \hat{i}_{sd} \quad (19)$$

$$e_{isq} = i_{sq} - \hat{i}_{sq} \quad (20)$$

## 2.2. Decoupling and Current Sensor

The direct-axis stator current  $i_{sd}$  (the rotor flux-producing component) and the quadrature-axis stator current  $i_{sq}$  (the torque-producing component) must be controlled separately for rotor flux-oriented vector control. The equations for the stator voltage components, on the other hand, are linked.  $u_{sd}$ , the direct axis component, and  $u_{sq}$ , the quadrature axis component, are both dependent on  $i_{sd}$ . For the rotor flux and electromagnetic torque, the stator voltage components  $u_{sd}$  and  $u_{sq}$  cannot be regarded as disconnected control variables. If the stator voltage equations are decoupled and the stator current components  $i_{sd}$  and  $i_{sq}$  are indirectly controlled by manipulating the induction motor's terminal voltages, the stator currents  $i_{sd}$  and  $i_{sq}$  can only be adjusted individually (decoupled control) [13]. The currents  $i_{sd}$  and  $i_{sq}$  are then controlled by Proportional Integral (PI) current sensor. The output current sensors are determined using equation [14]

$$u_{sd} = \left(K_{idp} + \frac{K_{idi}}{s}\right)(i_{sd}^* - i_{sd}) \quad (21)$$

$$u_{sq} = \left(K_{iqp} + \frac{K_{iqi}}{s}\right)(i_{sq}^* - i_{sq}) \quad (22)$$

where

$$i_{sd} = \frac{1}{T_d s + 1} i_{sd}^* \quad (23)$$

$$i_{sq} = \frac{1}{T_d s + 1} i_{sq}^* \quad (24)$$



### 2.1.3. Speed Controller

The reference current in  $q$ -reference frame ( $i_{sq}^*$ ) in (24) is controlled by the Integral Proportional (IP) speed controller. The equation of IP speed controller [15] is

$$i_{sq}^* = \int K_i (\omega_r^* - \omega_r) dt - K_p \omega_r \quad (25)$$

where  $K_p$  and  $K_i$  are the speed controller gain.

### 2.2. Testing Method

The system is tested using Matlab – Simulink – Cmx [16]. The simulation block diagram is shown in Figure 3.

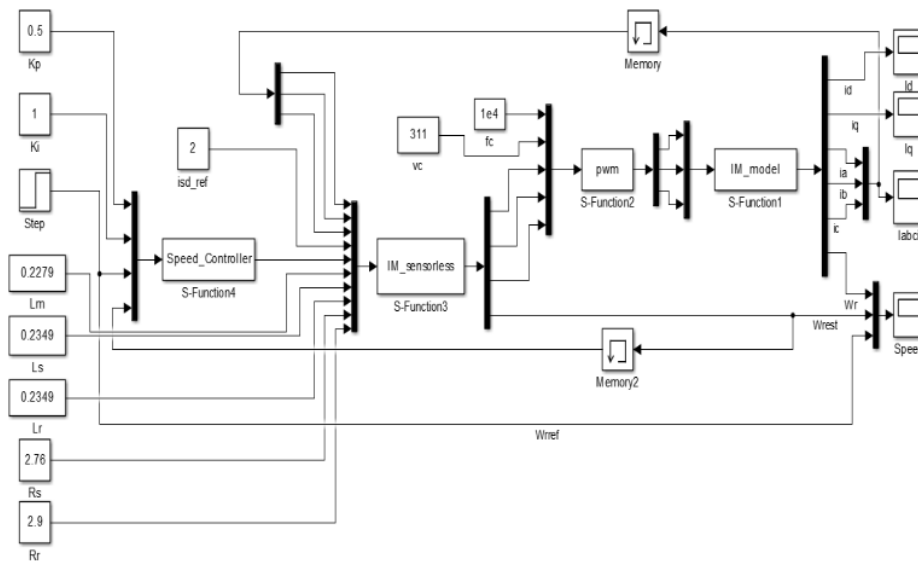


Figure 3. Simulation system

The values of the various parameters are inputted to the current controller using the input port in the figure. With the control parameters  $K_p=0.5$  and  $K_i=1$ , the reference speed is 100 rad/s. The stator and rotor resistance, stator and rotor inductance, and mutual inductance characteristics are all employed. In this test, the values of motor parameters in the controller vary as shown in Table 2, so they are different from the actual motor parameters.

**Table 2.** Variation Parameter Values of Induction Motor

Parameter	Percentage change (%)	Values	Unit
$R_s$	-50	1.38	$\Omega$
	-90	0.276	
	+50	4.14	
	+90	5.244	
$R_r$	-50	1.45	$\Omega$
	-90	0.29	
	+50	4.35	
	+65	4.785	
$L_s$	-4	0.225504	H
	-5	0.223155	
	+5	0.246645	
	+10	0.25839	
$L_r$	-4	0.225504	H
	-5	0.223155	
	+5	0.246645	
	+10	0.25839	
$L_m$	-2	0.223342	H
	-3	0.221063	
	-5	0.216505	
	-10	0.20511	
	+2.5	0.233598	
	+3	0.234737	

### 3 Results and Discussion

The simulation <sup>17</sup> result of the system using the right parameters is shown in Figure 4. It is shown that the actual speed ( $\omega_r$ ) can reach the reference speed ( $\omega_r^*$ ), i.e. 100 rad/s. <sup>16</sup> Although the estimated speed at the transient is slightly different from the actual speed, the estimated speed has the same value as the actual and reference speed at a steady-state. This means that the sensorless control system is working well. The simulation result of the system using various parameters values are described in Figures 5 - 9.

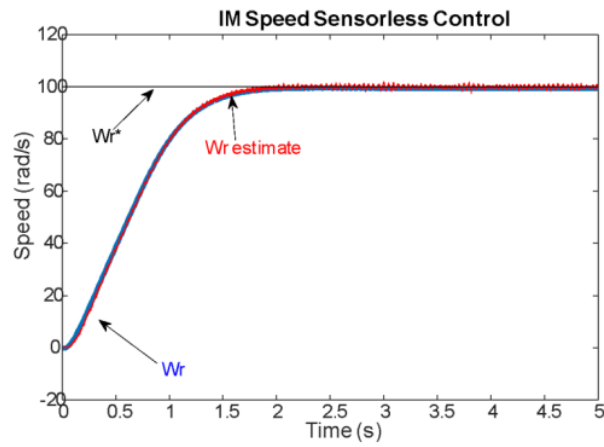


Figure 4. Simulation result with normal parameter values

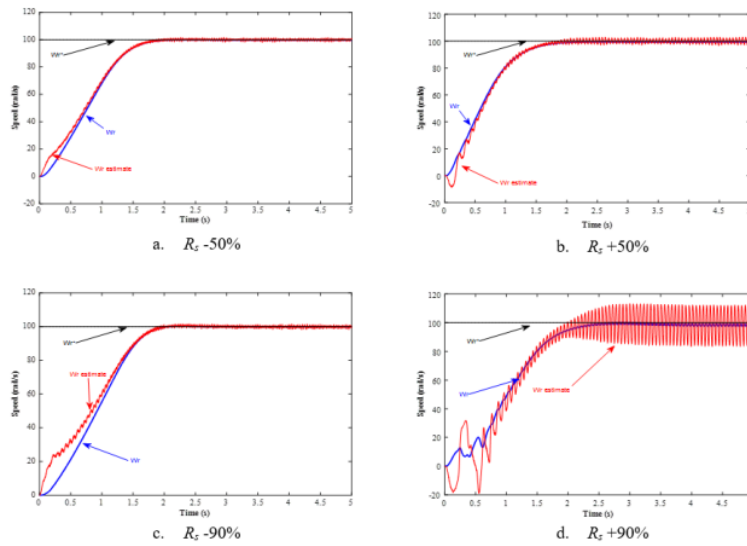
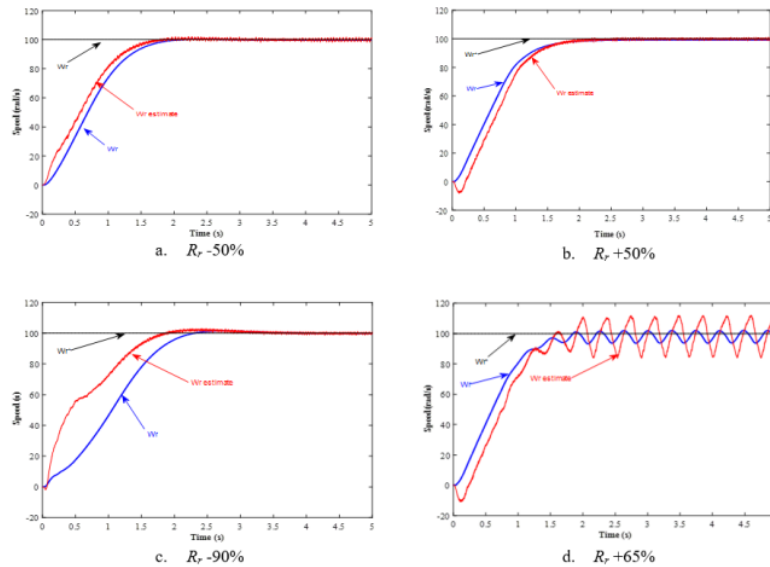


Figure 5. Simulation result with the variation of  $R_s$  parameter values

Figure 5 shows the value of  $R_s$  on the controller being varied. The figure shows that when the value of  $R_s$  in the controller is reduced to 90% (Figures 5.a and c), the actual speed can reach the reference speed, which is 100 rad/s, although there are differences in the transient conditions. When  $R_s$  is enlarged by 50% (Figure 5.b), the actual speed can

reach the reference speed, even though the estimated speed is oscillating. However, if the value of  $R_s$  is enlarged again, a steady state error occurs, where there is a difference between the actual and the reference speed, although only slightly (Figure 5.d). In this condition, the estimation speed oscillates with increasing amplitude. Thus, to get a good response, the difference in the value of  $R_s$  that can be applied is a maximum of +50%.



**Figure 6.** Simulation result with the variation of  $R_r$  parameter values

The condition for the change in the value of  $R_s$  is almost the same as the condition for the change in the value of  $R_r$ , as shown in Figure 6. The figure shows that when the value of  $R_r$  in the controller is reduced to 90% (Figures 6.a and c), the actual speed can reach the reference speed, namely 100 rad/s, although there is a difference in the transient conditions. In addition, when the  $R_r$  value is reduced, overshoot will occur (Figure 6.c), although the overshoot percentage is only slightly. When  $R_r$  is enlarged by 50% (Figure 5.b), the actual speed can reach the reference speed. However, if the value of  $R_r$  is enlarged again by 65%, the estimated speed and the actual speed oscillate (Figure 6.d). Thus, to get a good response, the difference in the value of  $R_r$  that can be applied is a maximum of 50%.

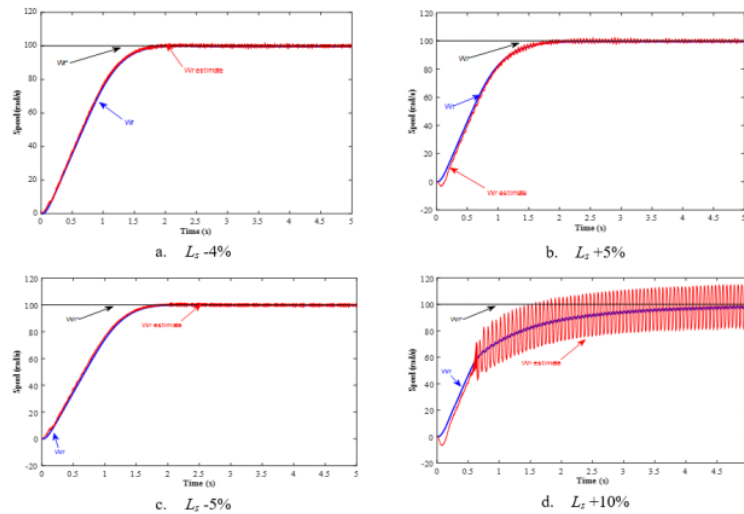


**Figure 7.** Simulation result with the variation of  $L_s$  parameter values

The effect of differences in resistance values is different from differences in inductance values, as illustrated in Figures 7 - 9. In the three figures, to get a good response, the difference in inductance values between the inductance values in the controller and the actual is very small. The difference in the values of  $L_s$  (Figure 7) and  $L_r$  (Figure 8) is between -5% to +5% (Figure 7.a - c and Figure 8.a -c). When the difference gets bigger, i.e. 10%, the estimation speed oscillates (Figs 7.d and 8.d). In the two figures, it appears that the actual speed time to achieve stability (settling time) is longer than before.

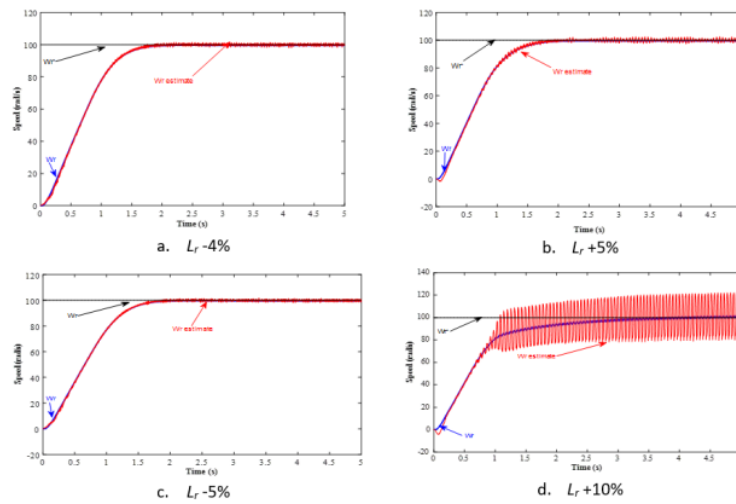


**Figure 8.** Simulation result with the variation of  $L_r$  parameter values

The small differences in the value of mutual inductance ( $L_m$ ) between the controller and the actual value of the motor parameters have greatly affected the system response, as illustrated in Figure 9. It appears that to get a good response, the differences in the inductance value between the inductance value in the controller and the actual is smaller than  $L_s$  and  $L_r$ . The difference in  $L_m$  values that can be applied is between -3% to +3% (Figure 9.a, c, d, f). As the difference gets bigger, the estimation speed oscillates (Figs 9.b and d). In the two figures, it appears that the actual speed time to achieve stability (settling time) is longer than before. When the  $L_m$  value is enlarged (more than +3%) the system becomes an error. Therefore, the recommended  $L_m$  differences value is -3% to +3%.

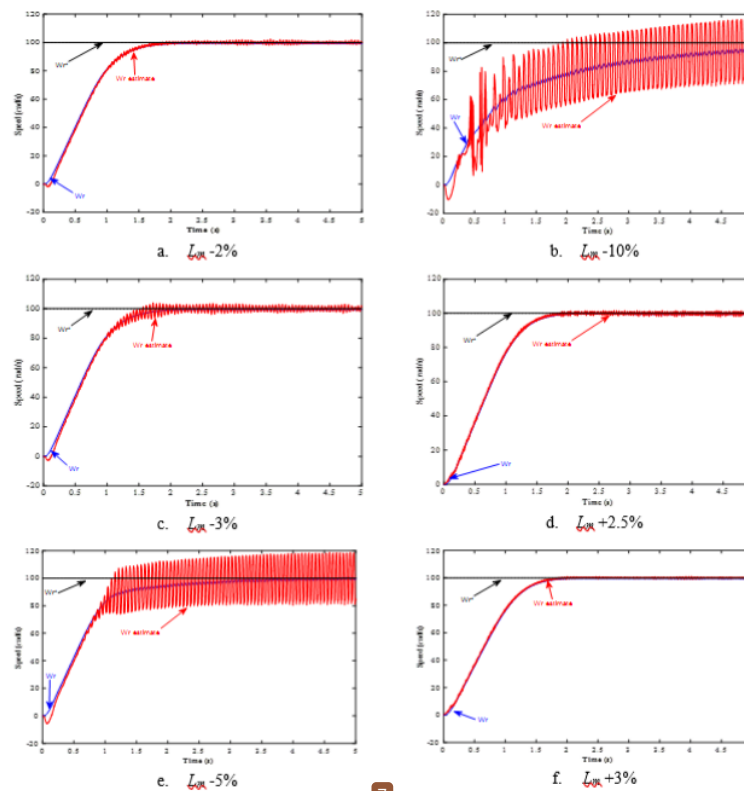


**Figure 9.** Simulation result with the variation of  $L_m$  parameter values

## 4 Conclusion

The differences in induction motor parameters between the controller and the actual value affect the system response. The value differences of  $R_r$  and  $R_s$  that can be applied are a maximum of 50%. However, the small differences in the inductance value greatly affect the system response. To get a good response, the value differences of  $L_s$  and  $L_r$  are between -5% to +5%, while the difference in the value of  $L_m$  is between -3% to +3%.

## References

- [1] Z. Alpholity X., S. S. Bhandari, P. P. Dsouza, and D. C. Raina, "Personal Assistant Robot," *Int. J. Appl. Sci. Smart Technol.*, **3**(2), 145–152, 2021.
- [2] Y. E. Loho, D. Lestariningsih, and P. R. Angka, "Alarm System and Emergency Message from Wheelchair User Emergency Condition," *Int. J. Appl. Sci. Smart Technol.*, **3**(2), 171–184, 2021.
- [3] B. W. Harini, F. Husnayain, A. Subiantoro, and F. Yusivar, "A synchronization loss detection method for PMSM speed sensorless control," *J. Teknol.*, **82**(4), 47–54, 2020.
- [4] P. Vas, *Sensorless Vector and Direct Torque Control*. Oxford University Press, 1998.
- [5] O. Avalos, E. Cuevas, and J. Gálvez, "Induction motor parameter identification using a gravitational search algorithm," *Computers*, **5**(2), 2016.
- [6] A. C. Megherbi, H. Megherbi, K. Benmahamed, A. G. Aissaoui, and A. Tahour, "Parameter identification of induction motors using variable-weighted cost function of genetic algorithms," *J. Electr. Eng. Technol.*, **5**(4), 597–605, 2010.
- [7] S. Yamamoto and H. Hirahara, "Effect of Parameter Tuning on Driving Performance of a Universal-Sensorless-Vector-Controlled Closed-Slot Cage Induction Motor," *2019 22nd Int. Conf. Electr. Mach. Syst. ICEMS 2019*, 2019.
- [8] Bernadeta Wuri Harini, "Pengaruh Parameter Motor pada Sistem Kendali tanpa Sensor Putaran," *J. Nas. Tek. Elektro dan Teknol. Inf.*, **10**(3), 236–242, 2021.
- [9] A. Glumineau and J. de León Morales, *Sensorless AC electric motor control*. Springer, 2015.
- [10] F. Yusivar and N. Avianto Wicaksono, "Simulasi Mesin Induksi Tanpa Sensor Kecepatan Menggunakan Pengendali Orientasi Vektor," *J. Nas. Tek. Elektro dan Teknol. Inf.*, **4**(4), 2016.
- [11] R. Ridwan, E. Purwanto, H. Oktavianto, M. R. Rusli, and H. Toar, "Desain Kontrol Kecepatan Motor Induksi Tiga Fasa Menggunakan Fuzzy Pid Berbasis Indirect Field Oriented Control," *J. Integr.*, **11**(2), 146–155, 2019.
- [12] J. Agrawal and S. Bodkhe, "Low speed sensorless control of PMSM drive using



- high frequency signal injection,” *12th IEEE Int. Conf. Electron. Energy, Environ. Commun. Comput. Control (E3-C3), INDICON 2015*, 4–9, 2016.
- [13] F. Semiconductor, “3-Phase AC Induction Motor Vector Control Using a 56F8300 Device,” *Memory*, 2005.
- [14] R. Gunawan and F. Yusivar, “Reducing estimation error due to digitizing problem in a speed sensorless control of induction motor,” *IECON Proc. (Industrial Electron. Conf.)*, **2005**(1), 1677–1682, 2005.
- [15] F. Yusivar, H. Haratsu, T. Kihara, S. Wakao, and T. Onuki, “Performance comparison of the controller configurations for the sensorless IM drive using the modified speed adaptive observer,” *IEE Conf. Publ.*, **475**, 194–200, 2000.
- [16] F. Yusivar and S. Wakao, “Minimum requirements of motor vector control modeling and simulation utilizing C MEX S-function in MATLAB/SIMULINK,” *Proc. Int. Conf. Power Electron. Drive Syst.*, **1**, 315–321, 2001.

This page intentionally left blank

# The Effect of Motor Parameters on the Induction Motor Speed Sensorless Control System using Luenberger Observer

---

## ORIGINALITY REPORT

---

12%

SIMILARITY INDEX

6%

INTERNET SOURCES

10%

PUBLICATIONS

4%

STUDENT PAPERS

---

## PRIMARY SOURCES

---

- |  |   |   |
|--|---|---|
| <div style="background-color: red; color: white; width: 40px; height: 40px; display: flex; align-items: center; justify-content: center; margin: 0 auto;">1</div>    | <p>Bernadeta Wuri Harini, Nanda Avianto, Feri Yusivar. "Effect of Initial Rotor Position on Rotor Flux Oriented Speed Permanent Magnet Synchronous Motor Control using Incremental Encoder", 2018 2nd International Conference on Smart Grid and Smart Cities (ICSGSC), 2018</p> <p>Publication</p> | <div style="font-size: 2em; font-weight: bold;">1</div> % |
| <hr/>  |   |   |
| <div style="background-color: purple; color: white; width: 40px; height: 40px; display: flex; align-items: center; justify-content: center; margin: 0 auto;">2</div> | <p>Bernadeta Wuri Harini, Aries Subianto, Feri Yusivar. "Stability analysis of MRAS speed sensorless control of permanent magnet synchronous motor", 2017 International Conference on Sustainable Energy Engineering and Application (ICSEEA), 2017</p> <p>Publication</p>                          | <div style="font-size: 2em; font-weight: bold;">1</div> % |
| <hr/>  |   |   |
| <div style="background-color: blue; color: white; width: 40px; height: 40px; display: flex; align-items: center; justify-content: center; margin: 0 auto;">3</div>   | <p>Submitted to College of Engineering, Pune</p> <p>Student Paper</p>   | <div style="font-size: 2em; font-weight: bold;">1</div> % |
| <hr/>  |   |   |
| <div style="background-color: teal; color: white; width: 40px; height: 40px; display: flex; align-items: center; justify-content: center; margin: 0 auto;">4</div>   | <p><a href="http://www.freescale.com">www.freescale.com</a></p> <p>Internet Source</p>  | <div style="font-size: 2em; font-weight: bold;">1</div> % |
-

5

Youssef Errami, Abdellatif Obbadi, Smail Sahnoun. "An improved control of grid integrated doubly fed induction generator", International Journal of Power and Energy Conversion, 2021

Publication

1 %

6

[journal.uad.ac.id](http://journal.uad.ac.id)

Internet Source

1 %

7

G. Rafajlovski, E. Ratz, D. Manov. "Modeling analysis and simulation of motor parameter variation in vector controlled electrical drives", Proceedings of Power Conversion Conference - PCC '97, 1997

Publication

1 %

8

R. Krishnan, Frank C. Doran. "Study of Parameter Sensitivity in High-Performance Inverter-Fed Induction Motor Drive Systems", IEEE Transactions on Industry Applications, 1987

Publication

1 %

9

Chukwuemeka N. Ibem, Mohamed Emad Farrag, Ahmed A. Aboushady. "Enhanced Fault Diagnosis of DFIG Converter Systems", 2019 54th International Universities Power Engineering Conference (UPEC), 2019

Publication

1 %

10

[journal.unnes.ac.id](http://journal.unnes.ac.id)

Internet Source

1 %

11

Alain Glumineau, Jesús de León Morales.  
"Sensorless AC Electric Motor Control",  
Springer Science and Business Media LLC,  
2015

Publication

1 %

12

Harini, Bernadeta Wuri, and Sri Agustini  
Sulandari. "The application of  
spectrophotometry method for measuring  
iron content of groundwater after Merapi  
Mountain eruption", 2013 International  
Conference on QiR, 2013.

Publication

<1 %

13

J. Theocharis, V. Petridis. "Neural network  
observer for induction motor control", IEEE  
Control Systems, 1994

Publication

<1 %

14

Murat Toren, Hakki Mollahasanoglu.  
"Determination of Optimum Stator and Rotor  
Resistance Values for Obtaining Parameters  
of Three Phase Induction Motor by Taguchi  
Method", 2021 13th International Conference  
on Electrical and Electronics Engineering  
(ELECO), 2021

Publication

<1 %

15 Phuc Thinh Doan, Thanh Luan Bui, Hak Kyeong Kim, Sang Bong Kim. "Sliding-mode observer design for sensorless vector control of AC induction motor", 2013 9th Asian Control Conference (ASCC), 2013  $<1\%$

---

Publication

16 Y. Takeda. "Sensorless control strategy for salient-pole PMSM based on extended EMF in rotating reference frame", Conference Record of the 2001 IEEE Industry Applications Conference 36th IAS Annual Meeting (Cat No 01CH37248) IAS-01, 2001  $<1\%$

---

Publication

17 ShuangHui Hao. "Research on closed-loop simulation system for digital AC servo system", Science in China Series E Technological Sciences, 07/2009  $<1\%$

---

Publication

18 [waseda.repo.nii.ac.jp](http://waseda.repo.nii.ac.jp)  $<1\%$

---

Internet Source

19 [www.datasheetarchive.com](http://www.datasheetarchive.com)  $<1\%$

---

Internet Source